A&A 380, 516–519 (2001)
DOI: 10.1051/0004-6361:20011390

Astronomy & Astrophysics

The gamma-ray source LSI +61°303

I. RXTE/ASM observations

D. A. Leahy*

Department of Physics, University of Calgary, Calgary, Canada T2N 1N4, Canada

Received 19 June 2001 / Accepted 1 October 2001

Abstract. An analysis of RXTE/ASM observations of the unusual binary system LSI +61°303 is presented. The X-ray light curve gives a binary period of 26.42 ± 0.05 days, and an eccentricity of 0.30 ± 0.04 (1σ). The eccentricity is determined by fitting an inverse Compton model to the X-ray light curve. These are the best determinations to date, as the optical period and eccentricity have larger uncertainties and published values of the radio period are variable. The radio outburst peak is not phase locked to the binary period, so the radio period is not the same as the binary period.

Key words. stars: neutron – stars: individual: LSI +61°303 – binaries: radio – stars: emission line, Be – X-rays: stars

1. Introduction

LSI +61°303 is one of a small but important group of radio emitting X-ray binary systems. The Be star LSI +61°303 is the optical counterpart of the periodic radio source GT 0236+610. The radio source is highly variable, exhibiting outbursts every 26.496 days which have rise times of ~1 day and last ~10 days (Gregory & Taylor 1978; Taylor & Gregory 1982). Two-frequency radio monitoring indicates a flat spectral index, and the emission has been interpreted as optically-thin synchrotron radiation for most of the outburst, with indication that the source becomes self-absorbed for a short time at the beginning of the outburst rise (Taylor & Gregory 1984). VLBI observations show that at its maximum size the emitting region has a dimension of $\sim 5\times10^{13}$ cm, and an expansion velocity (2.0–6.4) $\times10^{7}$ cm s^{-1} (Massi et al. 1993). The phase of peak flux varies between 0.4–1.0 of the radio ephemeris (phase 0 is arbitrarily defined as MJD 43366.275, with period 26.496 days), most often occurring at phase ~0.6 (Paredes et al. 1990; Ray et al. 1997). It has been suggested that the peak outburst flux is modulated on a four-year timescale (Gregory et al. 1989). Although it is evident that the peak radio flux is highly variable on timescales of several years, the four-year periodicity is not well established (Ray et al. 1997). Distance determinations place LSI +61°303 at 1.8–2.3 kpc (Gregory et al. 1979; Frail & Hjellming 1991).

Optical data show that the primary is a rapidly-rotating star of spectral type B0 V (Hutchings & Crampton 1981) or B0-B0.5 III (Paredes & Figueras 1986). Spectroscopic radial velocity measurements in the optical and UV confirm the binary nature of the system, and find an orbital period in agreement with that of the radio outbursts (Hutchings & Crampton 1981). The optical spectroscopic measurements of the system are however complicated by the composite and variable nature of the line emission (Hutchings & Crampton 1981), and have not yielded a good orbital solution. The best fit to these data imply a high-eccentricity of 0.6–0.8 and a periastron passage at radio phase of $\phi_{\rm p} \sim 0.2$, although the data is also consistent with zero eccentricity. Orbital solutions derived from infrared photometric observations also imply high eccentricities (0.7–0.8), with a best-fit periastron passage at $\phi_{\rm p} = 0.5$ (Marti & Paredes 1995). For this orbit and a Be star mass of 10 $M_\odot$ the semimajor axis of the orbit is 4–6 $\times10^{12}$ cm. Infrared measurements imply the presence of a dense equatorial disk, and a mass-loss rate in the wind of 1–4 $\times10^{-7}$ $M_\odot$ yr^{-1} has been estimated from these observations, assuming an opening angle of 15° for the disk and an initial wind velocity of 5 km s^{-1} (Waters et al. 1988).

Originally detected by Einstein, LSI +61°303 is a weak X-ray source, with $L_x \sim 10^{33}$ ergs s^{-1} (Bignami et al. 1981). ROSAT observations determined that the X-ray source is variable by a factor ~3 on timescales of a day, and has a harder spectrum than that characteristic of O and B stars

* e-mail: leahy@iras.ucalgary.ca

(Goldoni & Mereghetti 1995). Soft X-ray monitoring of LSI +61°303 with ROSAT at nine intervals during a single orbit showed the X-ray emission to be variable by a factor $\gtrsim$10 over the timescale of an orbit (Taylor et al. 1996). Simultaneous radio monitoring indicated that the X-ray and radio fluxes may be anti-correlated, which was confirmed by Harrison et al. 2000. *ASCA* observations (Leahy et al. 1997), show that the spectrum is described by a relatively hard power-law, and therefore the emission mechanism is non-thermal in nature.

LSI +61°303 is particularly interesting due to the fact that it is located within the error box of the strong 100 MeV COS B source 2CG 135+01 (Bignami & Hermsen 1983). Recent EGRET observations have narrowed the error region, and currently LSI +61°303 is the most probable X-ray counterpart (von Montigny et al. 1993). The luminosity in the EGRET band is $\sim 10^{35}$ (d/2 kpc)^2 erg s^{-1}. COMPTEL has also detected emission in the 1–10 MeV band from the same region (van Dijk et al. 1994) but the error circle also contains the quasar 4U 0241+61. RXTE/PCA and RXTE/HEXTE observations are presented by Harrison et al. (2000). These resolve LSI +61°303 from the QSO and show that COMPTEL flux is dominated by the QSO and not LSI +61°303. No significant variability has been detected in the high-energy data, however the observation periods are typically two weeks and thus sample a large fraction of the binary orbit.

In this paper, RXTE/ASM observations are analysed to give the orbital period, eccentricity and phase of periastron passage.

2. RXTE/ASM data analysis

The RXTE/ASM dwell data and daily-average data were obtained from the ASM web site (`http://xte.mit.edu/ASM_lc.html`). The data reduction to obtain the count rates and errors from the satellite observations was carried out by ASM/RXTE team, and the procedures are described at the web site. The ASM count rates are for the 1.5–12 keV keV band. The data covered the time period MJD 50088.1 to MJD 51969.2, or about 1881 days. Most of the RXTE/ASM data points are only upper limits to the source flux, with data values a factor of several less than the 1σ errors. However, when averaging over many points there is a flux significantly above zero. For example, averaging the data into 26.4 day bins yields 71 points: the mean ratio of count rate to 1σ error is 3.07, so that the source is well detected. In the next two subsections, it is found that the statistical significance of the periodicity found in power spectrum and epoch folding analysis is high. This is due to the large amount of data, even though each individual data point is of very low significance.

2.1. Power Spectrum Analysis

The power spectrum was created by averaging the dwell data into 0.05 day bins, subtracting the mean value of all inhabited bins from each inhabited bin, and taking an FFT. The dwell data were used in preference to the daily average data to avoid the effect of averaging over 1day intervals. Since the interest was only in periods greater than $\sim$1–2 days, and the sampling of the ASM data is poor on short timescales, the power spectrum was made with 4096 frequencies, 3.06×10^{-4}/day to 1.25/day. The resulting power at each frequency was divided by the average power over the whole frequency range. The χ^2 distribution was used to assess the significance of any peaks in the power spectrum. The most significant period was at 26.214 days, with a ratio of power/(mean power) of 12.09. This is statistically significant: the chance probability is 0.022 in 4096 trials. Also, the period is nearly the same as published values of the radio period. The period with next largest power was the adjacent period at 26.426 days. It had a ratio of power/(mean power) of 8.7, giving a chance probability of 0.68 in 4096 trials. This is not highly significant by itself, but with the above result confirms that there is a real periodicity in the data with a period between 26.2 and 26.4 days

2.2. Epoch folding analysis

An epoch folding analysis was carried out, with the χ^2 statistic used to assess the reality of variability at any given trial period. See Leahy et al. (1983) for a description of epoch folding and the assessment of period uncertainty. The daily-average data were folded into 24 phase bins in the period range of 20 days to 30 days, giving a maximum χ^2 of 66.6 and a chance probability of 5.0×10^{-4} at a period of 26.448 days. The dwell data were also epoch folded into 24 bins giving a maximum χ^2 of 103.6 and a chance probability of 8.6×10^{-10} at a period of 26.415 days. The epoch folding results from the dwell data are more significant than from the daily-average data. This is not surprising, the lower significance for the daily average data is probably due to the effect of averaging over 1 day intervals.

Other numbers of phase bins were also tried, since too many phase bins means too weak a signal in each bin, and too few phase bins results in smoothing the light curve. The optimum number of bins was determined by the maximum significance. Maximum χ^2 is not the correct discriminator, as the number of degrees of freedom (equal to number of bins less one) has a strong effect on the χ^2 probability distribution and is different for different numbers of bins. 10 bins gave a maximum χ^2 of 73.9 at 26.410 days and probability of 9.5×10^{-10}; 16 bins gave a maximum χ^2 of 93.4 at 26.415 days and probability of 6.0×10^{-11}; 32 bins gave a maximum χ^2 of 101.2 at 26.448 days and probability of 2.9×10^{-7}, Thus the maximum significance is obtained for folding into 16 phase bins. The χ^2 vs. period plot is given in Fig. 1 for 16 bins and two cases. A wide period range was folded at periods separated by 1/4 of the Nyquist frequency, and a narrow period range was folded at periods separated by 1/32 of the Nyquist frequency (the latter is offset by +80 in χ^2 to

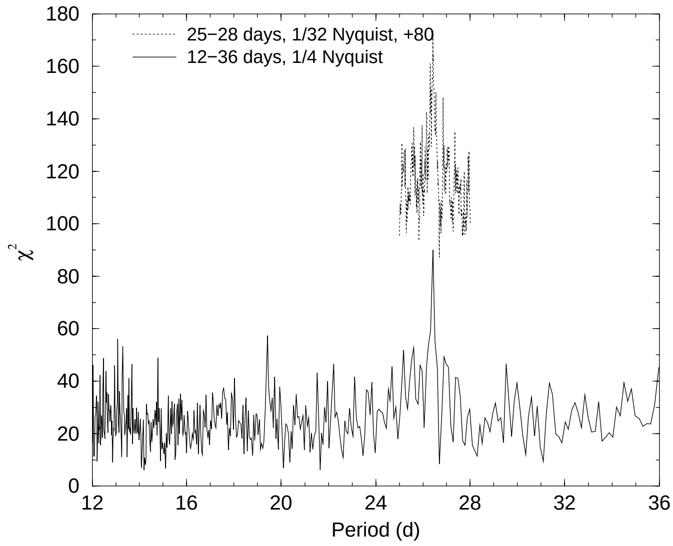

Fig. 1. Chisquared vs. period for the RXTE/ASM dwell data set folded into 16 phase bins. A wide period range folded at 1/4 Nyquist period spacing and a narrow period range folded at 1/32 Nyquist period spacing are shown (the latter has 80 added to χ^2 to avoid overlap).

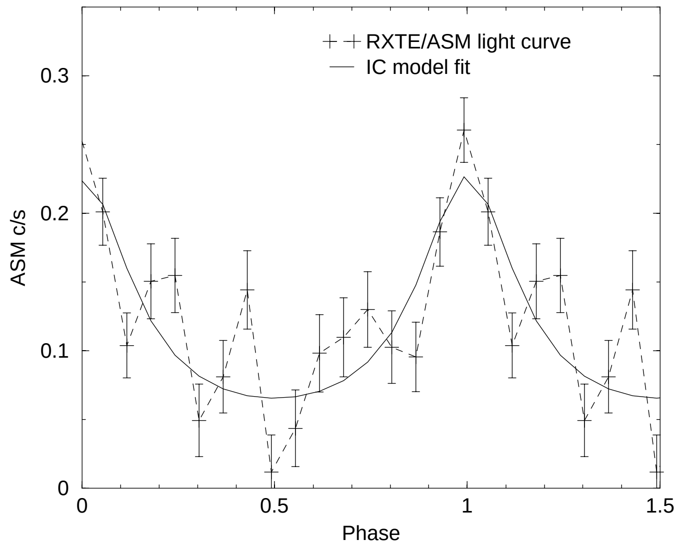

Fig. 2. Light curve at 26.415 days for the RXTE/ASM dwell data set folded into 16 phase bins. The solid line is the model fit described in the text.

avoid confusion of the two lines). The folded light curve at 26.415 days, the period of maximum χ^2, is shown in Fig. 2. The solid line is a model fit described below. The period uncertainty for the dwell data is ±0.05 days.

The dwell data were split into 6 adjacent sections and epoch folded, to test for period variability. There was 1 section of 269 days (MJD 50088.1 to 50357.1, chosen to be coincident with the time period used by Paredes et al. 1997), 4 sections of 300 days (MJD 50357.1 to 51557.1), and 1 section of 312 days (51557.1 to 51969.2). The period uncertainty was $\simeq$1.3 days: this is much larger than for the full data set due to both the weaker signal and shorter data span. All of the sections had maximum χ^2 from 35.2 to 52.6 and periods consistent with 26.4 days. Thus there is no evidence for period variability over the whole time period.

3. Discussion

The RXTE/ASM data consist the best long-term X-ray observations of LSI+61°303. The period determined here of 26.42 days is the best determination of the orbital period of this system. The uncertainty is dominated by the limit of the time span of observations and is ±0.05 day. The radio period shows evidence of being variable (e.g. see Ray et al. 1997), which is likely due to the radio outbursts not being tightly coupled to the orbital period. The optical period is the orbital period, but the only determination (Hutchings & Crampton 1981) has an uncertainty of ±0.1 days.

The X-ray light curve is produced by inverse Compton emission of stellar photons on the relativistic electrons responsible for the radio synchrotron emission (e.g. see Leahy et al. 1997). The peak of the X-ray emission should be consistently at periastron, unlike the radio emission peak which varies in phase. Thus the peak of X-ray emission and periastron occurs near phase 0.9. For the epoch folding analysis above, the reference for phase zero (T0x) was taken as MJD 50088.1.

To determine the phase of X-ray peak more accurately and also to estimate the eccentricity the inverse Compton model was fit to the light curve of Fig. 2. The best fit model is shown by the solid line. The resulting best fit eccentricity is 0.30 with a 1σ range of 0.26–0.34 and a 2σ range of 0.22–0.38. The eccentricity is consistent with the range ∼0.2–0.8 allowed by the optical observations (Hutchings & Crampton 1981). The best fit phase of periastron passage is 0.916 with a 1σ range of 0.90–0.93, and a 2σ range of 0.89–0.95. This yields the epoch of periastron passage of MJD 50112.3 ± 0.8 (2σ).

The average radio lightcurve was used to define phase 0 as peak radio flux in Ray et al. 1997 to yield a reference epoch of JD 2449393.5(±0.4). Taylor & Gregory (1984) defined phase 0.6 as peak radio flux to yield a reference epoch of JD 2443366.775. The resulting phase of radio outburst for the two different radio epochs are at phase, with reference to T0x, $0.69 \pm .06$ and 0.1 ± 0.5. The uncertainty is primarily due to the uncertainty in the X-ray period, but the difference is due to the different periods and epochs published for radio outburst. So rather than using mean period and epoch for radio outburst, it is preferable to consider cases where radio and X-ray have been observed together. Two orbital cycles which have been sampled by observations with ROSAT and RXTE simultaneous with radio monitoring (Harrison et al. 2000). These both have the radio outburst occuring ∼0.4 in orbital phase after X-ray peak.

The basic nature of the system LSI +61°303 is now thought to be as follows: electrons are accelerated to relativistic energies probably by a pulsar in orbit around the

Be star primary star. The acceleration mechanism could be electromagnetic fields in the vicinity of the pulsar or shock acceleration at the boundary of the pulsar outflow and the stellar wind from the primary. The flux of stellar photons interacts with the power law distribution of relativistic electrons to produce a broad power law distribution of photons from X-ray through γ-ray energies. Due to the magnetic field in the vicinity of the pulsar, the same electrons radiate synchrotron photons in the 1 GHz to >100 GHz range. The eccentric orbit of the pulsar and its associated relativistic electron population result in the moderate modulation of the X-ray through γ-ray flux. The radio outburst is much more highly variable than the X-ray and is not phase locked with the orbit. The radio outburst follows the X-ray peak by $\sim$0.4 in orbital phase, so that the radio outburst occurs approximately near apastron. The radio outburst emission has been successfully described as due to a rapidly expanding cloud of relativistic electrons (Peracaula 1997).

4. Summary

The RXTE/ASM has monitored LSI +61°303 for a significant amount of time now (over 5 years). Here the dwell data and daily-average data were analyzed to study the orbital light curve and long term light curve of LSI +61°303. An epoch folding analysis gives a binary period of 26.42 ± 0.05 days. The inverse Compton emission mechanism for the X-ray emission was originally suggested by Maraschi & Treves (1981), and confirmed by detailed modeling of the multiwavelength spectrum by Leahy et al. (1997). Fitting the inverse Compton model to the X-ray light curve yields the eccentricity of 0.30 ± 0.04 (1σ), ± 0.08 (2σ). These are the best determinations of orbital period and eccentricity yet for LSI +61°303.

Further work including a detailed model of the radio through γ-ray emission, with several new features beyond that presented in Leahy et al. (1997), is presented in a following paper.

Acknowledgements. This paper made uses of the quick-look results provided by the ASM/RXTE team. DAL acknowledges support from the Natural Sciences and Engineering Research Council.

References

Bignami, G. F. B., Caraveo, P. A., Lamb, R. C., Markert, T. H., & Paul, J. A. 1981, ApJ, 247, L85
Bignami, G. F. B., & Hermsen, W. 1983, ARA&A, 21, 67
Frail, D. A., & Hjellming, R. M. 1991, AJ, 101, 2126
Goldoni, P., & Mereghetti, S. 1995, A&A, 299, 751
Gregory, P. C., & Taylor, A. R. 1978, Nature, 272, 704
Gregory, P. C., Xu, H. J., Backhouse, C. J., & Reid, A. 1989, ApJ, 339, 1054
Gregory, P. C., Taylor, A. R., Crampton, D., et al. 1979, AJ, 84, 1030
Harrison, F., Ray, P., Leahy, D., Waltman, E., & Pooley, G. 2000, ApJ, 528, 454
Hutchings, J. B., & Crampton, D. 1981, PASP, 93, 486
Leahy, D. A., Elsner, R. F., & Weissskopf, M. C. 1983, ApJ, 272, 256
Leahy, D., Harrison, F., & Yoshida, A. 1997, ApJ, 475, 823
Maraschi, L., & Treves, A. 1981, MNRAS, 194, 1P
Marti, J., & Paredes, J. M. 1995, A&A, 269, 249
Massi, M., Paredes, J. M., Estalella, R., & Felli, M. 1993, A&A, 269, 249
Paredes, J., Marti, J., Peracaula, M., & Ribo, M. 1997, A&A, 320L, 25
Paredes, J. M., Estalella, R., & Rius, A. 1990, A&A, 232, 377
Paredes, J. M., & Figueras, F. 1986, A&A, 154, L30
Peracaula, M. 1997, Ph.D. Thesis, University of Barcelona
Ray, P., Foster, R., Waltman, E., Tavani, M., & Ghigo, F. 1997, ApJ, 491, 381
Taylor, A. R., & Gregory, P. C. 1982, ApJ, 255, 210
Taylor, A. R., Young, G., Peracaula, M., Kenny, H. T., & Gregory, P. C. 1996, A&A, 305, 817
Taylor, A. R., & Gregory, P. C. 1984, ApJ, 283, 273
van Dijk, R., Bloemen, H., Hermsen, W., et al. 1994, in The Evolution of X-ray Binaries (New York: AIP Press), 324
von Montigny, C., Brazier K., Kanbach, G., et al. 1993, IAU Circ., 5708
Waters, L. B. F. M., van den Heuvel, E. P. J., Taylor, A. R., Habets, G. M. H. J., & Persi, P. 1988, A&A, 198, 200